

a periodic effect and is due to the fact that Cr is a group 6 metal while Co, Fe, and Ni are group 8 metals.

This study provides a guide based on bond order, structure, and reactivity for additional studies on the ion-molecule chemistry of the ionic cluster fragments. Currently, we are examining the ion-molecule chemistry of heteroatom ionic cluster fragments (e.g., Co/Ni, Cr/Ni, Fe/Ni, Cr/Fe, Co/Fe, and Co/Cr) to probe further the relationship between the CVM theory and the reaction sequence of the ionic cluster fragments.

In addition, more detailed studies on ligand effects are underway. In these studies we are comparing the cluster formation sequences of ions such as  $MH^+$ ,  $MCO^+$ , and  $MNO^+$ . Studies

with these and additional ligand systems are designed to investigate ligand effects on the nature of the ionic cluster fragments formed and the influence of the initial ligand on the degree of coordination unsaturation of the ionic cluster fragment product ions.

**Acknowledgment.** This work was supported by the U.S. Department of Energy, Office of Basic Energy Sciences (DE-A505-82ER13023). Some of the TAMU Equipment was purchased from funds provided by the TAMU Center for Energy and Mineral Resources. We gratefully acknowledge the Texas Agriculture Experimental Station which provided a fraction of the funds for purchase of the Nicolet FTMS 1000 spectrometer.

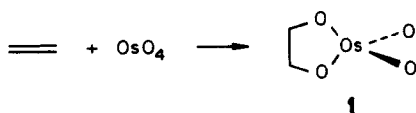
## Binding of Alkenes to the Ligands in $OsO_2X_2$ ( $X = O$ and $NR$ ) and $CpCo(NO)_2$ . A Frontier Orbital Study of the Formation of Intermediates in the Transition-Metal-Catalyzed Synthesis of Diols, Amino Alcohols, and Diamines

Karl Anker Jørgensen and Roald Hoffmann\*

Contribution from the Department of Chemistry, Baker Laboratory, Cornell University, Ithaca, New York 14853. Received July 31, 1985

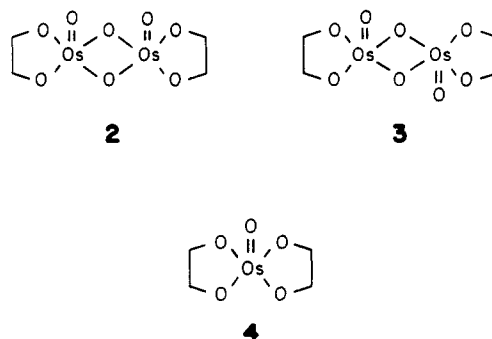
**Abstract:** The concerted  $[3 + 2]$  cycloaddition of an alkene to the oxygen ligands in osmium tetroxide and the binding of the alkene to the metal center leading to an asymmetric intermediate are analyzed from the frontier orbital point of view. It is suggested that the increased reactivity of osmium tetroxide with alkenes in the presence of tertiary amines, e.g., pyridine, follows from a *cis* addition of pyridine to osmium tetroxide, leading to a geometrical distortion of the osmium tetroxide fragment from  $T_d$  to an activated  $C_{2v}$  symmetry. The calculations are supported by the structure of the products. The reactions of  $d^0$  bis(imido)oxoosmium species with alkenes are examined in a similar way. The reactions of a seemingly very different, yet in fact similar ( $\eta^5$ -cyclopentadienyl)dinitrosocobalt complex have also been analyzed from a frontier orbital point of view. The valence MO's are constructed from the cobalt dinitrosyl cation and cyclopentadienyl anion. The structure of the nitrosyl groups (bent or linear) is studied, and it has been found that the bent structure has the lowest energy. The binding of alkenes to the nitrosyl ligands is examined.

The reaction of alkenes with osmium tetroxide to form *cis*-diols is an old and well-established reaction.<sup>1</sup> The reaction takes place via an osmium(VI) intermediate, **1**, which on reductive or oxidative hydrolysis yields the corresponding *cis*-diol. The osmium(VI)



intermediate is usually written as a tetrahedral species, **1**.<sup>2</sup> Although it may exist as a transient complex in solution, tetrahedral **1** would be unlikely to be stable in the solid state, as it is a tetrahedral  $d^2$  complex; there are few examples of tetrahedral  $d^2$  stereochemistry for third-row transition metals.<sup>3</sup> In nonreducing solvents, alkenes ( $R$ ) react with osmium tetroxide to give products of stoichiometry  $OsO_4 \cdot R$  and  $OsO_5 \cdot R_2$ .<sup>4</sup> These products

have recently been found to be dimeric monoester complexes, *syn*- and *anti*- $[Os_2O_4(O_4R)_2]$  (**2** and **3**), and monomeric diester complexes,  $[OsO(O_2R)_2]$  (**4**).<sup>5</sup>



The initial addition of osmium tetroxide is accelerated by tertiary bases, especially pyridine.<sup>6</sup> The molecular structures of

(1) (a) Makowka, O. *Chem. Ber.* **1908**, *41*, 943. (b) See e.g.: March, J. "Advanced Organic Chemistry"; McGraw-Hill: New York, 1977; p 748. And: Fieser, L. F.; Fieser, M. "Reagents for Organic Synthesis"; Wiley, New York, 1985; Vol. 1-6.

(2) (a) Cotton, F. A.; Wilkinson, G. "Advanced Inorganic Chemistry", 3rd ed.; Interscience: New York, 1972; p 1003. (b) House, H. O. "Modern Synthetic Reactions", 2nd ed.; Benjamin: San Francisco, CA, 1972; p 277.

(3) (a) Schroder, M. *Chem. Rev.* **1980**, *80*, 187. (b) The Sharpless group has recently characterized such an adduct from  $Os(NR)_4$  and dimethyl fumarate, private communication.

(4) (a) Criegee, R. *Ann.* **1936**, *522*, 75; *Angew. Chem.* **1937**, *50*, 153; **1938**, *51*, 519.

(5) (a) Marzilli, L. G.; Hanson, B. E.; Kistenmacher, T. J.; Epps, L. A.; Steward, R. C. *Inorg. Chem.* **1976**, *15*, 1661. (b) Collin, R. J.; Jones, J.; Griffith, W. P. *J. Chem. Soc., Dalton Trans.* **1974**, 1094. (c) Phillips, F. L.; Skapski, A. C. *Ibid.* **1975**, 2586. (d) Phillips, F. L.; Skapski, A. C. *Acta Crystallogr., Sect. B* **1975**, *31*, 1814. (e) Collins, R. J.; Griffith, W. P.; Phillips, F. L.; Skapski, A. C. *Biochem. Biophys. Acta* **1973**, *320*, 745. (f) Collins, R. J.; Griffith, W. P.; Phillips, F. L.; Skapski, A. C. *Ibid.* **1974**, *354*, 152.

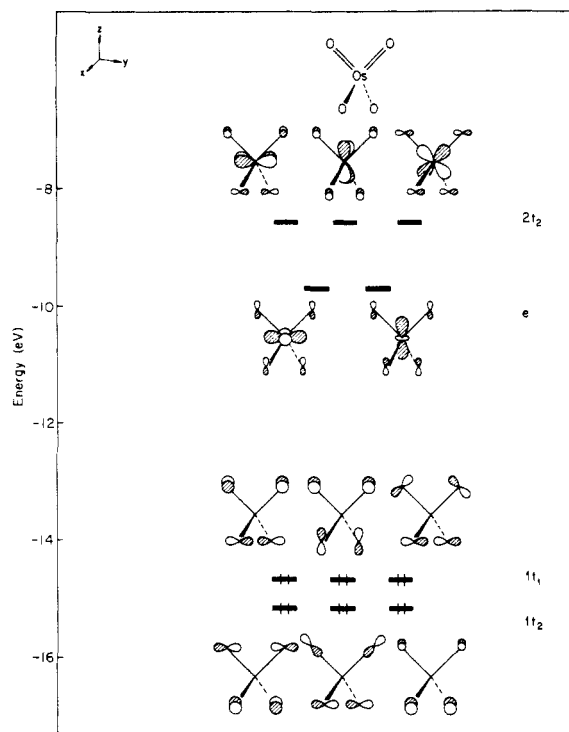
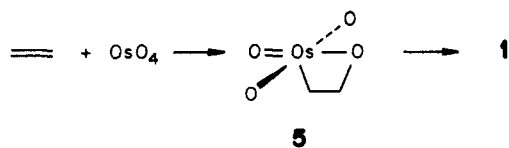


Figure 1. Valence orbitals of  $\text{OsO}_4$ .

some  $\alpha,\alpha'$ -(dipyridine)osmate(VI) esters (two pyridines coupled to the osmium atom) and the  $\alpha$ -quinuclidine)osmate(VI) ester of cyclohexene (one pyridine coordinated to the osmium atom) have been elucidated by X-ray diffraction.<sup>7</sup>

The mechanism for the formation of **2-4** has in general been thought to involve direct attack of the oxygens at the unsaturated carbons, to form the cyclic intermediate. Sharpless and co-workers<sup>8</sup> have recently suggested an alternative mechanism: the carbon in the  $\text{C}=\text{C}$  bond, which is a weak nucleophile, might attack the more electropositive osmium to give an asymmetric organometallic intermediate **5** which rearranges to intermediate **1**. The proposed asymmetric intermediate **5** has also been sug-



gested as a useful explanation for the increase in the rate of formation of the osmium(VI) ester complexes on addition of tertiary amines, such as pyridine.<sup>8,3a</sup> Recently there has been some discussion about the NMR experimental evidence for the formation of an asymmetric intermediate in the oxidation of alkenes by osmium tetroxide.<sup>9</sup>

$d^0$  alkylimido transition-metal species are known as compounds of a series of transition metals.<sup>10,11</sup> Reactions of bis(*N-tert*-bu-

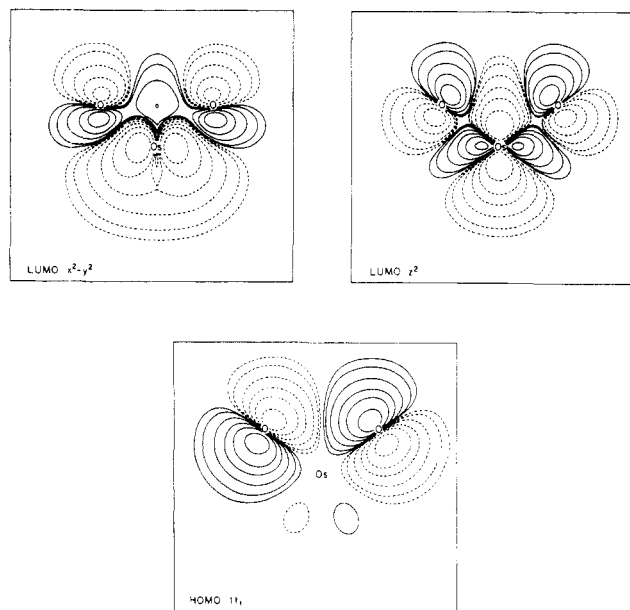
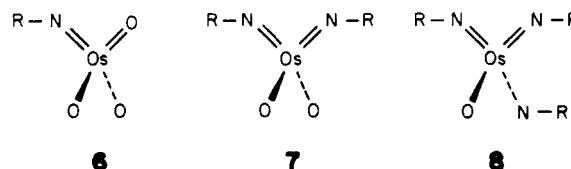


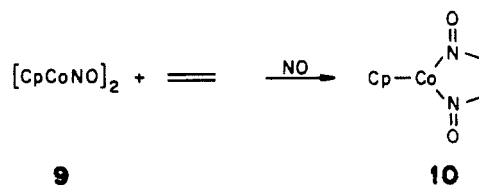
Figure 2. Plot of three of the valence orbitals of  $\text{OsO}_4$ . The contour levels of  $\Psi$  are 0.2, 0.1, 0.055, 0.025, 0.01, and 0.005. The orbitals are plotted in the  $yz$  plane. The two upper plots are the LUMO's and the lower the HOMO.

tylimido)tetroxoosmium(VIII) complexes, **6**, and alkenes have recently been studied by Sharpless and co-workers,<sup>11d,e,12</sup> who found the 1,2-amino alcohols as the primary products, with the diols as byproducts. They have also found that they could increase the



amino alcohol-diol ratio by addition of pyridine and certain tertiary alkyl bridgehead amines.<sup>11d,e,12</sup> Similar diamino- and triaminoosmium complexes, **7** and **8**, respectively, have been found to produce the 1,2-diamine by reaction with alkenes.<sup>11d,e</sup>

Let us turn to a seemingly very different yet, as we will argue, closely related reaction. A ( $\eta^5$ -cyclopentadienyl)(dinitroso)cobalt complex **9**, has also been shown to react with alkenes, yielding the corresponding dinitrosoalkanes **10**.<sup>13</sup> **10** can be reduced with  $\text{LiAlH}_4$  to give the primary 1,2-diamine.<sup>13</sup>



Organometallic reactions of alkenes can be divided in two types. The large majority proceed by a classical type of mechanism:  $\pi$  coordination of the alkene by the metal center followed by an insertion and then a reductive elimination (eq 1a). The second type of mechanism has been noted in a smaller number of cases.

(6) Criegee, R.; Marchand, B.; Wannowius, H. *J. Liebigs Ann.* **1942**, 550, 99.

(7) (a) Conn, J. F.; Kim, J. J.; Suddath, F. L.; Blattmann, P.; Rich, A. *J. Am. Chem. Soc.* **1974**, 96, 7152. (b) Kistenmacher, T. J.; Marzilli, L. G.; Rossi, M. *Bioinorg. Chem.* **1976**, 6, 347. (c) Neidle, S.; Stuart, D. L. *Biochem. Biophys. Acta* **1976**, 418, 226. (d) Cartwright, B. A.; Griffith, W. P.; Schröder, M.; Skapski, A. C. *J. Chem. Soc., Chem. Commun.* **1978**, 853. (e) Schröder, M.; Nielson, A. J.; Griffith, W. P. *J. Chem. Soc., Dalton Trans.* **1979**, 1607.

(8) (a) Sharpless, K. B.; Teranishi, A. Y.; Bäckvall, J.-E. *J. Am. Chem. Soc.* **1977**, 99, 3120. (b) Hentges, S. G.; Sharpless, K. B. *Ibid.* **1980**, 102, 4263.

(9) (a) Schröder, M.; Constable, E. C. *J. Chem. Soc., Chem. Commun.* **1982**, 734. (b) Casey, C. P. *Ibid.* **1983**, 123.

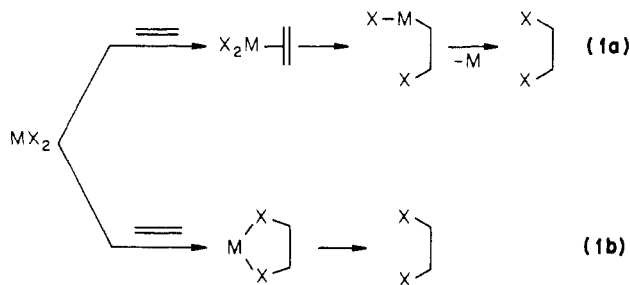
(10) (a) Slawisch, V. A. *Z. Anorg. Allg. Chem.* **1970**, 374, 291. (b) Shihada, V. A. F. *Ibid.* **1974**, 408, 9.

(11) (a) Clifford, A. F.; Kobayashi, C. S. *Abstr. Pap.—Am. Chem. Soc.* **1956**, 58, 50R. (b) Rochow, E. G. *Inorg. Synth.* **1960**, 6, 207. (c) Milas, N. A.; Iliopoulos, M. I. *J. Am. Chem. Soc.* **1959**, 81, 6089. (d) Sharpless, K. B.; Patrick, D. W.; Truesdale, L. K.; Biller, S. A. *J. Am. Chem. Soc.* **1975**, 97, 2305. (e) Chong, A. O.; Oshima, K.; Sharpless, K. B. *Ibid.* **1977**, 99, 3420. (f) Nugent, W. A.; Haymore, B. L. *Coord. Chem. Rev.* **1980**, 31, 123. (g) Nugent, W. A.; Harlow, R. L.; McKinney, R. J. *J. Am. Chem. Soc.* **1979**, 101, 7265.

(12) (a) Patrick, D. W.; Truesdale, L. K.; Biller, S. A.; Sharpless, K. B. *J. Org. Chem.* **1978**, 43, 2628. (b) Hentges, S. G.; Sharpless, K. B. *Ibid.* **1980**, 45, 2257.

(13) (a) Becker, P. N.; Bergman, R. G. *Organometallics* **1983**, 2, 787. (b) Becker, P. N.; Bergman, R. G. *J. Am. Chem. Soc.* **1983**, 105, 2985.

The ligands are here activated by the metal bound to them so that the alkene reacts directly at the ligands (eq 1b).



Our primary goal in this paper is to present a coherent theoretical model that allows one to understand the observed reactivity and intermediates. For these purposes, symmetry arguments and extended Hückel calculations are used.<sup>14</sup>

We begin with osmium tetroxide, which has  $T_d$  symmetry.<sup>15</sup> The frontier orbitals are shown in Figure 1, and the energy levels show the expected splitting, with the occupied MO's of  $t_1$  and  $t_2$  symmetry and the unoccupied MO's of  $e$  and  $2t_2$  symmetry. The occupied MO's of  $t_1$  and  $t_2$  symmetry are 2p AO's on oxygen, whereas the unoccupied MO's of  $e$  and  $2t_2$  symmetry are mainly 5d orbitals on osmium mixed in with a small amount of 2p on oxygen. Note the anticipated  $e$  below  $t_2$  splitting of the d block of a tetrahedral complex. Contour plots of the three orbitals of osmium tetroxide which might be expected to be involved in a  $[3 + 2]$  cycloaddition reaction are shown in Figure 2. In order to anticipate the further discussion of the interaction of these orbitals with  $\pi$ -type donors and/or acceptors, it is appropriate to comment here on the nature of these two  $e$  and one of the  $1t_1$  orbitals. The  $e$  orbitals are mainly  $z^2$  and  $x^2-y^2$  mixed with 2p on oxygen, in which the AO's on the oxygens, in the  $yz$  plane, have  $p_z$  character and are symmetric with respect to the  $xz$  plane. The  $1t_1$  orbital is a combination of p orbitals on the upper oxygens, a mixture of  $p_z$  and  $p_y$  locally in this coordinate system and antisymmetric with respect to the  $xz$  plane. These orbitals are set up for an interaction with the symmetric and antisymmetric  $\pi$  orbitals, respectively, of an alkene.

The observed order of the valence orbitals in  $\text{OsO}_4$  is in accordance with other calculations.<sup>16</sup>

Let us try to analyze a model for formation of the asymmetric intermediate **5**. The first step in such a reaction might then be a symmetric complex of the alkene and osmium tetroxide, approaching **1**. One could also envisage a slipping of the osmium tetroxide fragment along the alkene, eventually giving the asymmetric intermediate **5**. A related slipping motion has been postulated for a transition-metal activation of an alkene toward intermolecular nucleophilic attack.<sup>17</sup>

From the shape of the frontier orbitals of osmium tetroxide, it looks as if it is the oxygens which are best set up for an interaction with the alkene, as we have here an interaction of the LUMO ( $\pi^*$ ) of an alkene with one of the HOMO's of osmium tetroxide ( $1t_1$ ) and an interaction of the  $\pi$  HOMO of the alkene with one of the LUMO's of  $e$  symmetry of osmium tetroxide. In the case of an asymmetric intermediate, the only effective interaction is between the HOMO of the alkene and the  $z^2$  LUMO orbital of osmium tetroxide. Both reactions will be investigated below. The reader may be interested in a study by DuBois et al.,<sup>18</sup> in which similar frontier orbital arguments are used to discuss the interaction of alkenes with bridging sulfur atoms in dinuclear complexes.

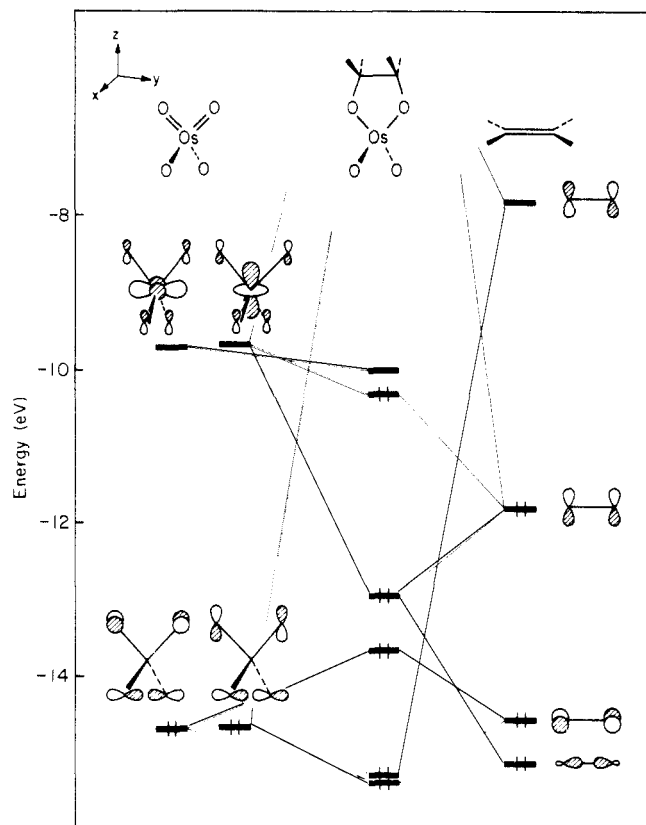


Figure 3. Interaction diagram for the formation of the osmium ester complex **11** from osmium tetroxide and ethylene.

As a model for osmium ester complexes **2-4**, we have used structure **11** where the bond lengths and angles are taken from ref 5b. An interaction diagram for the formation of **11** from osmium tetroxide and ethylene fragments is shown in Figure 3.

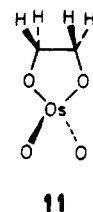


Figure 3 shows the energy levels and wave functions for osmium tetroxide on the left or for ethylene at the right. In the center are the energy levels of the product of the reaction, which has  $C_{2v}$  symmetry. Only these orbitals which interact strongly and thus change in energy are shown in this interaction diagram. Thus, many oxygen lone pairs and four of the metal d block orbitals are omitted.

The LUMO of  $\text{OsO}_4$  is of  $e$  symmetry (see Figure 1). The primary interaction is of the  $z^2$  component of this LUMO, with ethylene  $\sigma$  and  $\pi$  lower-lying symmetric oxygen lone-pair combinations also getting involved in a complicated mixing pattern. The resultant HOMO of **11** is again mainly  $z^2$ , mixed in with a small amount of  $x^2-y^2$  and  $\pi$ . Note that the reaction is formally a reduction at the metal. Thus, one moves from the situation of no metal d orbitals formally occupied to one such primarily d function populated,  $\text{Os}(\text{VIII}), d^0 \rightarrow \text{Os}(\text{VI}), d^2$ .

It may be noted that the cycloadduct HOMO,  $z^2$ , is lower than it was in the reactant  $\text{OsO}_4$  (where it was unfilled). The reason for this is the loss of  $\pi$  antibonding in this  $z^2$ , as two oxygen lone pairs are converted to CO bonds. Similar  $\pi$  effects have been identified as important in oxidation and metathesis reactions by Goddard and co-workers.<sup>19</sup>

(14) Hoffmann, R. *J. Chem. Phys.* **1963**, *39*, 1397.

(15) Ueki, T.; Zalkin, A.; Templeton, D. H. *Acta Crystallogr.* **1965**, *19*, 157.

(16) (a) Foster, S.; Felps, S.; Cusachs, L. C.; McGlynn, S. P. *J. Am. Chem. Soc.* **1973**, *95*, 5521. (b) Rauk, A.; Ziegler, T.; Ellis, D. E. *Theoret. Chim. Acta* **1974**, *34*, 49.

(17) (a) Eisenstein, O.; Hoffmann, R. *J. Am. Chem. Soc.* **1980**, *102*, 6148.

(b) Eisenstein, O.; Hoffmann, R. *Ibid.* **1981**, *103*, 4308.

(18) DuBois, D. L.; Miller, W. K.; Rakowski DuBois, M. *J. Am. Chem. Soc.* **1981**, *103*, 3429-3436.

(19) Rappé, A. K.; Goddard, W. A., III. *Nature (London)* **1980**, *285*, 311; *J. Am. Chem. Soc.* **1980**, *102*, 5114; **1982**, *104*, 3287.

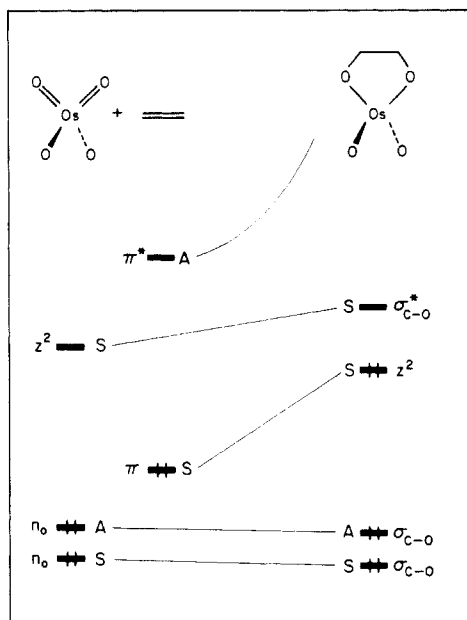
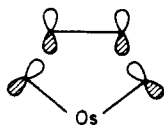


**Figure 4.** Schematic correlation diagram for the reaction of osmium tetroxide and ethylene.

One of the oxygen lone-pair,  $t_1$  combinations of  $\text{OsO}_4$ , anti-symmetric with respect to the vertical plane, is stabilized by interaction with ethylene  $\pi^*$ . This may be seen in Figure 3 at the bottom. The net reaction appears to be an allowed one. This may be seen in the schematic correlation diagram of Figure 4. Only the essential orbitals are shown: the ethylene  $\pi$ , and  $\pi^*$ , on  $\text{OsO}_4$  two oxygen lone pairs and the  $z^2$  LUMO. Note the correlation of  $\pi$  of ethylene with  $z^2$  of Os. This is not an "easy" correlation but takes place through a complex series of mixings and avoided crossings.

In fact, the classification of the reaction as an allowed one is probably not appropriate—it is better to call it a metal-catalyzed forbidden reaction. Among the symmetric orbitals there is one, the antibonding mixture of  $n_O$  and ethylene  $\pi$ , shown in **12**, whose



**12**

intent is to correlate with a  $\sigma^*_{\text{CO}}$  combination. But as this level rises in energy, it encounters (and cannot cross) the Os  $z^2$ . An avoided crossing results, which prevents the reaction from attaining its intended very high activation energy. The metal has catalyzed the reaction by providing a home for two potentially antibonding electrons and by allowing itself to be reduced. Figure 5, in showing the way the energy levels evolve along the reaction path, illustrates clearly the intended and avoided crossing mentioned above.

Though the crossing is avoided, a high activation energy still results. The reaction is indeed slow. The LUMO orbital in **11** is mainly of  $z^2-y^2$  character on the osmium atom, which is consistent with attack of nucleophiles at this site at the metal as in the hydrolysis of the osmium ester<sup>20</sup> complexes.

It is known that alkenes undergo oxidative cleavage of the double bond by ruthenium tetroxide.<sup>21</sup> From the present calculations, it is not possible to make a clear distinction between the osmium ester complex **11** and a similar ruthenium ester complex; there is only a slight difference in overlap population

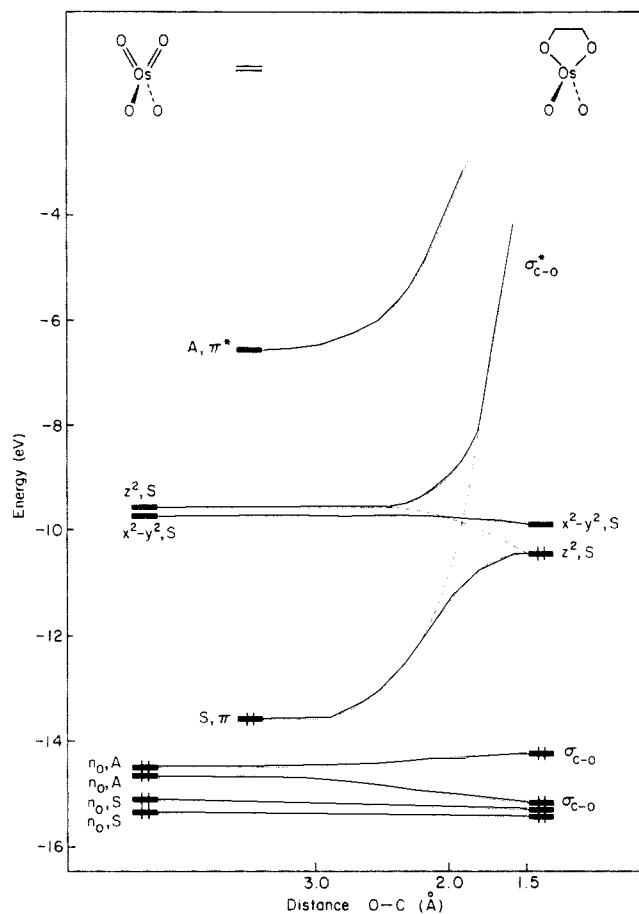


**Figure 5.** Evolution of the energy levels of osmium tetroxide and ethylene along the reaction path.

in the two complexes—not enough to account for their different chemical behavior.

It is not possible from an orbital argument to distinguish between the symmetric osmium ester complex **11** and the asymmetric **5**, as the latter has  $C_s$  symmetry. But different factors appear to us to favor the [3 + 2] cycloaddition reaction between osmium tetroxide and alkenes over a competing [2 + 2] cycloaddition reaction: As mentioned earlier, the frontier orbitals in osmium tetroxide are set up for a [3 + 2] cycloaddition reaction, whereas a geometric distortion of osmium tetroxide would have to take place if the reaction were a [2 + 2] cycloaddition reaction, followed by a second deformation back to the symmetric osmium ester complex **11**. Perhaps this might be expected to be unfavorable due to the principle of least motion. So, in the following, attention will be focused mainly on a concerted mechanism, although one cannot rule out on theoretical grounds the mechanism proposed by Sharpless.

Let us now proceed to the reaction of osmium tetroxide with alkenes in the presence of tertiary amines. Much interest has been devoted to these reactions, since pyridine provides a marked increase in reaction rate.<sup>3,6</sup> The effect has been used to support the argument for an asymmetric intermediate.<sup>3,8</sup> It is our intention in the following to propose an alternative. We will study distortions in the geometry of osmium tetroxide caused by the pyridine ligands followed by [3 + 2] cycloaddition, in an attempt to explain the increased reactivity and observed structure of the products.

From kinetic experiments, both complexes of the  $\alpha$ -pyridyl and  $\alpha, \alpha'$ -dipyridylosmium tetroxide type have been suggested,<sup>20,22</sup> but it has been noted that although the stability constant of the latter complex is small, the rate of reaction with an alkene is much

(20) Subbaraman, L. R.; Subbaraman, J.; Behrman, E. J. *Inorg. Chem.* **1972**, *11*, 2621.

(21) See e.g.: March, J. "Advanced Organic Chemistry"; McGraw-Hill: New York, 1977; p 1095.

(22) (a) Clark, R. L.; Behrman, E. J. *Inorg. Chem.* **1975**, *14*, 1425. (b) Clark, R. L.; Behrman, E. J. *Bioinorg. Chem.* **1971**, *1*, 35. (c) Jencks, W. P. "Catalysis in Chemistry and Enzymology"; McGraw-Hill: New York, 1969; pp 574, 602.

Scheme I

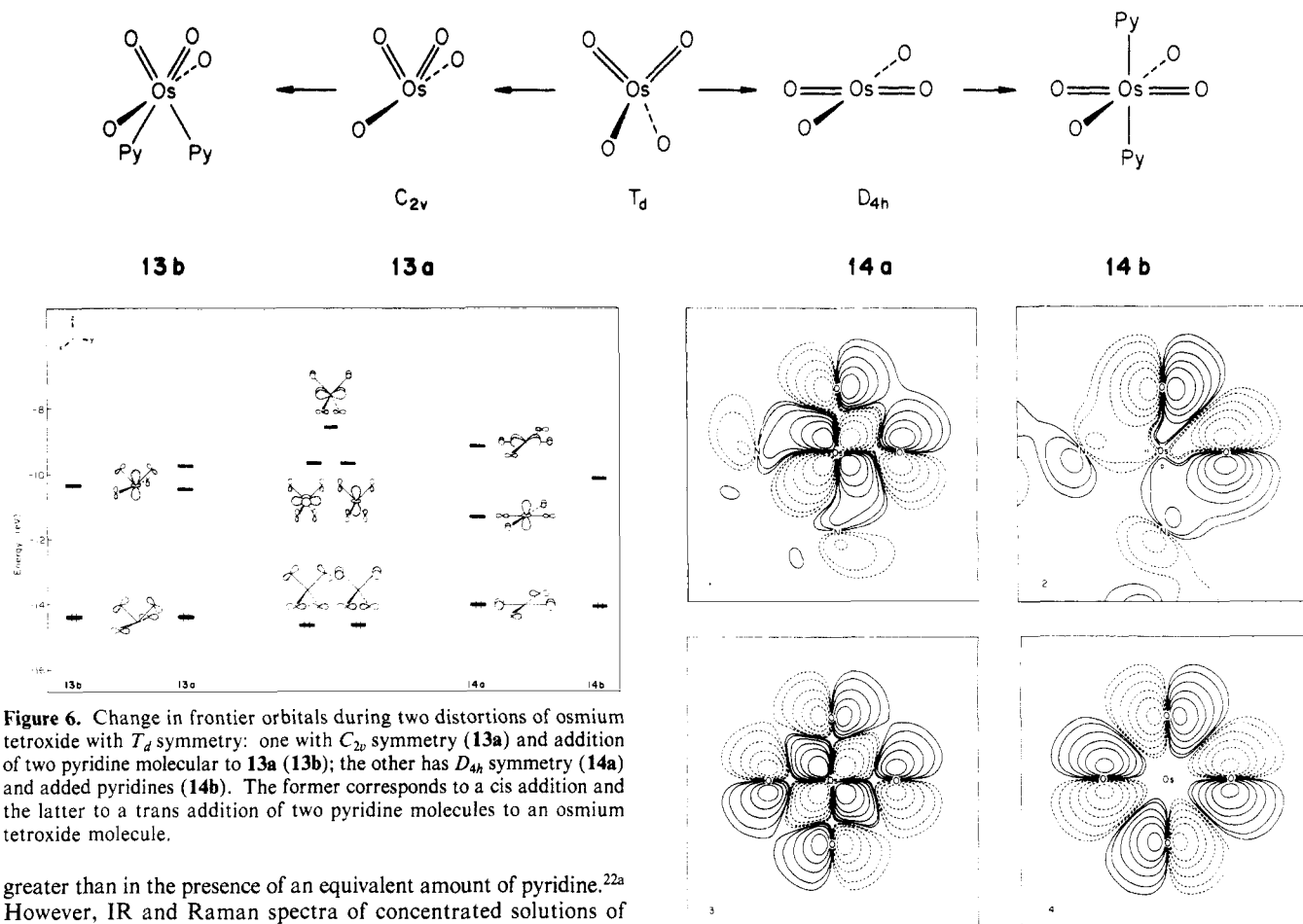


**Figure 6.** Change in frontier orbitals during two distortions of osmium tetroxide with  $T_d$  symmetry: one with  $C_{2v}$  symmetry (**13a**) and addition of two pyridine molecular to **13a** (**13b**); the other has  $D_{4h}$  symmetry (**14a**) and added pyridines (**14b**). The former corresponds to a cis addition and the latter to a trans addition of two pyridine molecules to an osmium tetroxide molecule.

greater than in the presence of an equivalent amount of pyridine.<sup>22a</sup> However, IR and Raman spectra of concentrated solutions of osmium tetroxide and pyridine show no bands other than those attributable to  $\text{OsO}_4$ ,  $\text{OsO}_4\cdot\text{py}$ , and pyridine.<sup>23</sup>

A  $\text{ML}_4$  fragment with  $T_d$  symmetry can easily be transformed into other structures by geometrical distortions.<sup>24</sup> We have decided here to study two geometrical distortions of osmium tetroxide: one leading to osmium tetroxide with  $D_{4h}$  symmetry, which might be formed from a trans interaction of the lone pair at the pyridine nitrogen with the LUMO orbital of osmium tetroxide with  $z^2$  character (**14a** and **b** in Scheme I); the other leading to osmium tetroxide with  $C_{2v}$  symmetry, which might be formed from a similar cis interaction, probably with the LUMO orbital with  $x^2-y^2$  character (**13a** and **b** in Scheme I).

The changes in the frontier orbitals during these distortions ( $\text{OsO}_4 \rightarrow \mathbf{13a}$  and  $\mathbf{13b}$  and  $\text{OsO}_4 \rightarrow \mathbf{14a}$  and  $\mathbf{14b}$ ) are shown in Figure 5. Only the orbitals which might be expected to interact with an alkene are included. The Os-N (nitrogen in pyridine) has been found to optimize in our calculations at about 2.2 Å in **13b** and **14b**, and this bond length is in accordance with experimental results.<sup>7a-c</sup>

It appears from Figure 6 that the HOMO energy level which has the right symmetry for an interaction with the  $\pi^*$  orbital in an alkene is constant during the transformation to **13a** and **13b**, whereas it increases about 0.5 eV during the transformation to **14a** and **14b**, because of the out-of-phase interaction between the cis oxygens. The e component with  $z^2$  character in  $T_d$  osmium tetroxide is stabilized by about 0.6 eV during the distortion to  $C_{2v}$  symmetry (**13a**) and addition of pyridine (**13b**), whereas the energy of the other e symmetry orbital (the one with  $x^2-y^2$  character) increases by interaction with the lone-pair electrons of the pyridine nitrogen. By the distortion to  $D_{4h}$  symmetry (**14a**), one of the e levels ( $z^2$ ) is stabilized and the other ( $x^2-y^2$ ) destabilized. One of the  $2t_1$  levels ( $xy$ ) in  $T_d$  osmium tetroxide is stabilized both

**Figure 7.** Plot of the valence orbitals of **13b** and **14b** which can be involved in an addition to alkenes. 1 and 2 are the active orbitals in similarly for 3 and 4 in **14b**. For contours, see Figure 2. The plane is  $xy$ .

by the distortion to  $D_{4h}$  symmetry and by the trans addition of two pyridines and now becomes the LUMO of **14b**, because the LUMO of **14a** ( $z^2$ ) is sharply destabilized by its interaction with lone-pair electrons of nitrogen in pyridine.

Contour plots of the orbitals of **13b** and **14b** in Figure 6 are shown in Figure 7.

Using a frontier orbital line of reasoning, i.e., the energy term from the second-order perturbation theory,<sup>25</sup>

$$\Delta E \propto \frac{|H_{ij}|^2}{E_i - E_j} \quad (2)$$

and the results shown in Figure 6, it appears that both osmium tetroxide-pyridine complexes, **13b** and **14b**, should be more reactive with the  $\pi$  and  $\pi^*$  orbitals in an alkene, compared with osmium tetroxide. The increased reactivity comes mainly from a decrease in the energy difference, in the denominator of eq 2, because of a smaller  $\epsilon_{\text{HOMO(alkene)}} - \epsilon_{\text{LUMO(13b,14b)}}$  and  $\epsilon_{\text{HOMO(13b,14b)}} - \epsilon_{\text{LUMO(alkene)}}$  difference. Furthermore,  $|H_{ij}|^2$  in eq 2 increases for both **13b** and **14b** because the molecular orbital coefficients for both reactive levels in these complexes are bigger than in the corresponding orbitals in osmium tetroxide.

This might be the explanation for the observed increase in reactivity, but from the present results it is not possible to distinguish between a reaction path taking place via a  $C_{2v}$  or  $D_{4h}$  osmium tetroxide-pyridine complex, as the total one-electron energies of **13b** and **14b** are of about the same size. In attempts

(23) Griffith, W. P.; Rossetti, R. J. Chem. Soc., Dalton Trans. 1972, 1449.

(24) Elian, M.; Hoffmann, R. Inorg. Chem. 1975, 14, 1058.

(25) See e.g.: Fujimoto, H.; Fukui, K. In "Chemical Reactivity and Reaction Paths"; Klopman, G., Ed.; Wiley: New York, 1974; p 23.

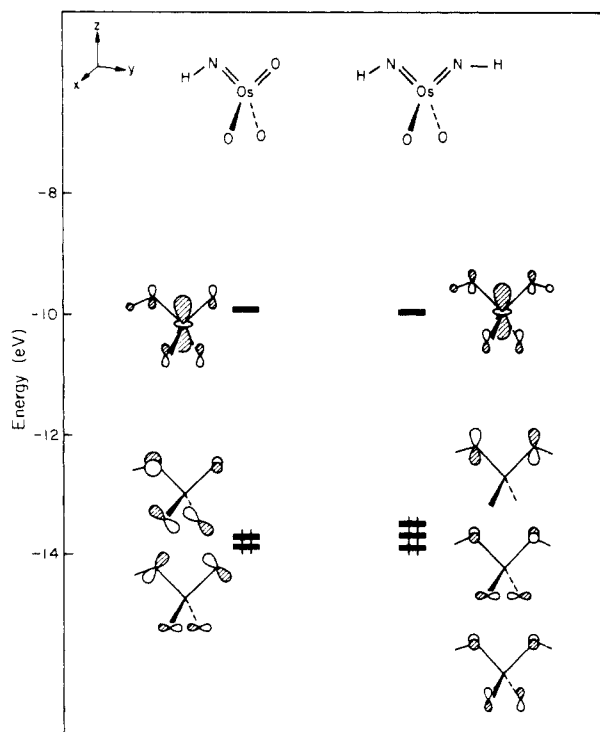
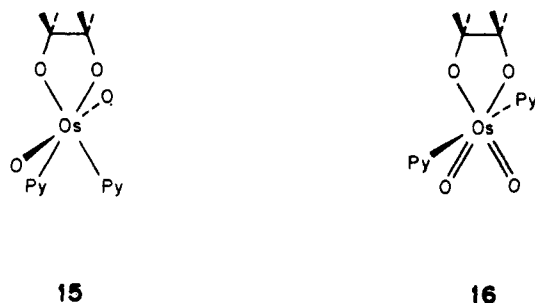


Figure 8. Valence orbitals of  $\text{OsO}_3\text{NH}$  (left) and  $\text{OsO}_2\text{N}_2\text{H}_2$  (right).

to find the reaction path, we have calculated the total energy for the products, **15** and **16**, obtained in a reaction between **13b** and **14b** and ethylene, respectively. These calculations give **15** as the



most stable compound by about 1 eV, which is in accordance with the structure found by X-ray crystallographic investigations.<sup>7a-c</sup> Thus, we suggest that the pyridine-catalyzed reaction probably takes place via a  $C_{2v}$  osmium tetroxide-pyridine complex.

A 1:1 adduct between osmium tetroxide and quinuclidine has been isolated and characterized by X-ray crystallographic investigations. The structure is trigonal-bipyramidal: one of the oxygens and quinuclidine are axial, and the remaining three oxygens are equatorial.<sup>26</sup> Calculations on trigonal-bipyramidal geometry of osmium tetroxide indicate a similar pattern of the frontier orbitals as outlined in Figure 4—a [3 + 2] cycloaddition of the alkene to the oxygens of osmium tetroxide should follow. The osmium tetroxide-quinuclidine adduct reacts with cyclohexene to give an asymmetric bridged ester complex.<sup>7d,26</sup>

Let us continue with the  $d^0$  bis(imido)oxoosmium species **6** and **7**. Figure 8 shows the basic orbitals of **6** and **7** (with  $R = \text{H}$ ).

It appears from the left part of Figure 8 that the orbital components both on the two lower oxygens and the nitrogen and upper oxygen in the LUMO of  $\text{OsO}_3\text{NH}$  have correct symmetry for an interaction with the symmetric  $\pi$  orbital in an alkene. The HOMO, however, has only the lower oxygens set up to interact with the antisymmetric alkene  $\pi^*$  orbital. The nitrogen and upper oxygen components do not have the right shape for an interaction

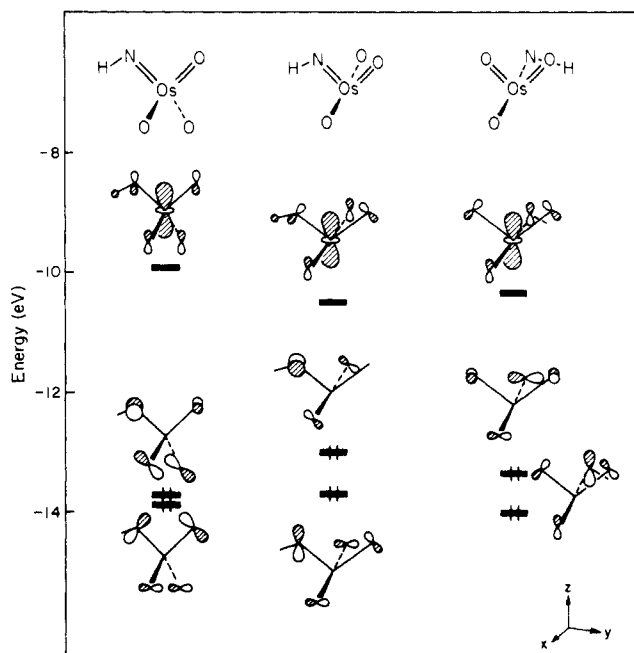


Figure 9. Valence orbitals of **6**, **6a**, and **6b**.

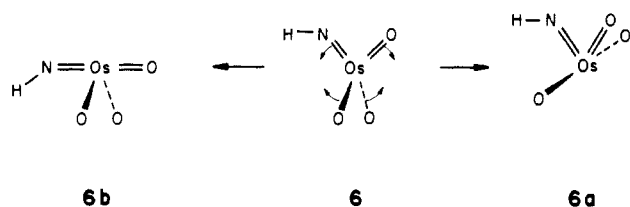
(these are of  $p_x$  character). In the second HOMO, located 0.15 eV below the first, the pattern is reversed: the nitrogen and upper oxygen might be able to interact with the LUMO of an alkene, whereas this is not possible for the two lower oxygens. For the orbitals with mainly  $p_z$  character, the electron densities in the MO's are as follows: LUMO, lower oxygens 0.130, nitrogen and upper oxygen 0.197; HOMO, lower oxygens 0.309; second HOMO, nitrogen and upper oxygen 1.772. It appears from the LUMO numbers that these give about the same contribution to  $|H_{ij}|^2$  and thus the same contribution to  $\Delta E$ , when only the interaction with the symmetric  $\pi$  orbital in an alkene is considered. In the interaction with the antisymmetric  $\pi$  orbital, however, it might be expected that the second HOMO, which is composed mainly of  $p_z$  orbitals on nitrogen and the upper oxygen, will be most important. This is because of the large orbital coefficient there compared with the components on the lower oxygens in the HOMO, even though this level is located 0.15 eV above the second HOMO. Further evidence for preferred binding of an alkene to oxygen and nitrogen, rather than to two oxygens, comes from calculation of the total one-electron energy of possible products, which gives the former as the most stable.

Besides the electronic effect operating in this type of reaction, a steric effect might also be involved. In the calculations, a hydrogen has been used as the R group on the nitrogen, whereas in the experiments *t*-Bu and 1-adamantyl groups are used.<sup>11d,12</sup> These bulky groups might reverse the binding of the alkene from nitrogen-oxygen to oxygen-oxygen in certain reactions where large steric interactions between the R group on nitrogen and parts of the substrate are possible. This has also been observed in some reactions where a noncoordinating solvent is used.<sup>11d</sup>

As in the osmium tetroxide reactions, solvent also plays an important role in the oxyamination process, and it has been observed that in all the cases studied where a particular alkene was oxyaminated in methylene chloride and in pyridine, reactions carried out in pyridine gave consistently higher yields of the amino alcohol and less diol.<sup>11d,12</sup> Let us try to analyze this observation by using a geometrical distortion of **6**. On the basis of the results obtained for the pyridine-catalyzed osmium tetroxide reaction and the observation that the amines normally form *cis*-osmium complexes,<sup>27</sup> a " $C_{2v}$ -like" distortion of **6** is studied. There are two possible  $C_{2v}$ -like structures of **6**: **6a** and **6b**. The valence orbitals of **6**, **6a**, and **6b** are shown in Figure 9.

(26) Griffith, W. P.; Skapski, A. C.; Woode, K. A.; Wright, M. J. *Inorg. Chem. Acta* **1978**, *31*, L413.

(27) See Adams, R. D.; Selegne, J. P. In "Comprehensive Organometallic Chemistry"; Wilkinson, G., Ed.; Pergamon Press: London **1985**; Vol. 4, p 82 and references therein.



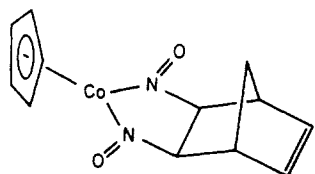
By the geometric distortion of **6** to **6b**, the LUMO is stabilized because of the loss of destabilizing  $\pi$  bonding with  $z^2$ . However, both the first and second HOMO levels are destabilized, probably because the out-of-phase overlap between the p orbitals of the two lower oxygens with the p orbitals on nitrogen and the upper oxygen increases. A similar pattern is observed for **6b**. When the symmetry of the main parts of the MO coefficients of the two sets of frontier orbitals in **6a** and **6b** is compared, it appears that **6a** has the best orbitals for an interaction with an alkene. Both have, with respect to the  $xz$  plane, a symmetric  $p_y$ - $p_z$  and antisymmetric  $p_x$ - $p_z$  combination of the LUMO and second HOMO. But the density of the active orbitals in **6a** is much higher compared with **6b**; the LUMO of **6a** is located lower and the second HOMO of **6a** is located higher relative to **6b**, which might account for the observed oxyamination when pyridine is present.<sup>11d,12</sup>

It should also be pointed out that in both cases, interaction between atoms in other planes will also be possible, but these will probably only play a minor role due to the relatively low MO coefficients in these planes.

Let us finish the discussion of osmium complexes with the frontier orbitals of the diaminoosmium species **7**, shown in Figure 8 at the right. The LUMO is symmetric and is of  $z^2$  character, mixed in with some p character on the nitrogens and oxygens. The HOMO is of  $p_z$  character located on the nitrogens and is antisymmetric with respect to the  $xz$  plane. The antisymmetric orbital on the oxygens is located as the third HOMO. From the frontier orbitals with mainly  $p_z$  character, which are able to interact with the  $\pi$  orbitals of an alkene, the electron density in the MO's is as follows: LUMO, nitrogens, 0.246; oxygens, 0.112; HOMO, nitrogens, 1.826; third HOMO, oxygens, 0.133. It appears that it is the nitrogens which probably will have the preferred interaction with the HOMO and LUMO of an alkene. This follows from the large electron density on the nitrogens compared with the oxygens in the LUMO. Probably these considerations account for the appearance of osmium(VI) diamino complexes as the main products in these reactions.<sup>11e</sup>

### Cobalt-Based Amination

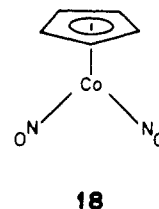
The synthesis of primary 1,2-diamines from alkenes can be achieved by binding the alkene to the nitrosyl ligands in a ( $\eta^5$ -cyclopentadienyl)dinitrosylcobalt complex,  $\text{CpCo}(\text{NO})_2$ , followed by reduction.<sup>13</sup> X-ray crystallographic investigations of the product obtained in the reaction between  $\text{CpCo}(\text{NO})_2$  and norbornadiene reveal that the nitrogens bind to the carbons in the alkene,<sup>28</sup> **17**.



17

In this reaction the alkene binds to the nitrosyl nitrogen, which can be compared to the binding to imido nitrogens in the bis-(imido)dioxosmium(VIII) complexes, **7**. Let us proceed with a study of the structure of  $\text{CpCo}(\text{NO})_2$  and how alkenes bind to it. A suitable starting point for this analysis is to construct the

valence MO's of a  $\text{CpCo}(\text{NO})_2$ , **18**, with linear nitrosyl ligands,



18

from an interaction between the MO's of the fragments constituting the complete molecule, here a  $\text{Co}(\text{NO})_2^+$  moiety and the  $\text{C}_5\text{H}_5^-$  ligand. Figure 10 shows the interaction diagram for the construction of the MO's of  $\text{CpCo}(\text{NO})_2$ ; at the left are the valence orbitals of  $\text{Co}(\text{NO})_2^+$ , at the right  $\text{C}_5\text{H}_5^-$ , and in the middle the product.

The orbitals of  $\text{Co}(\text{NO})_2^+$  are typical of a  $d^{10}$   $\text{ML}_2$  fragment, except that the  $\pi^*$  orbitals of a nitrosyl are so low in energy that some are interspersed with the metal d block. This complication persists in the composite  $\text{CpCo}(\text{NO})_2$  complex. If the nitrosyls are linear and counted as  $\text{NO}^+$ , this is a 20-electron complex. No wonder a level high above a nice gap is filled. This is an antibonding combination of  $2b_2$  of  $\text{Co}(\text{NO})_2^+$  with  $e_1''$  of  $\text{C}_5\text{H}_5^-$  and is illustrated in Figure 10. At this point, there is no real reason to single out this orbital, for three other low-lying orbitals are near it. But this orbital will turn out to be the only one effective in the subsequent reaction with an ethylene.

The HOMO wave function of  $\text{CpCo}(\text{NO})_2$  is shown in Figure 11.

We have here studied  $\text{CpCo}(\text{NO})_2$  as if it were a "planar" molecule (at Co), but it is expected to have a "pyramidal" geometry.<sup>29</sup> However, let us continue with a planar geometry, for reasons which will become clear.

Several different structures of  $\text{CpCo}(\text{NO})_2$  are possible. Bergman and Becker have suggested three interesting possibilities:<sup>13</sup> **18a-c**. One is the 20-electron species, **18a**. Two energetically favorable 18-electron systems have also been proposed: an  $\eta^3$ - $\text{C}_5\text{H}_5$  ( $\pi$ -allyl) species, **18b**, and one in which one of the nitrosyls is bent, **18c**. We will add to these three structures a fourth one, **18d**; in this species both nitrosyls are bent. This gives the molecule a symmetry plane, but as it is a 16-electron system, it might be energetically less favorable than the others.

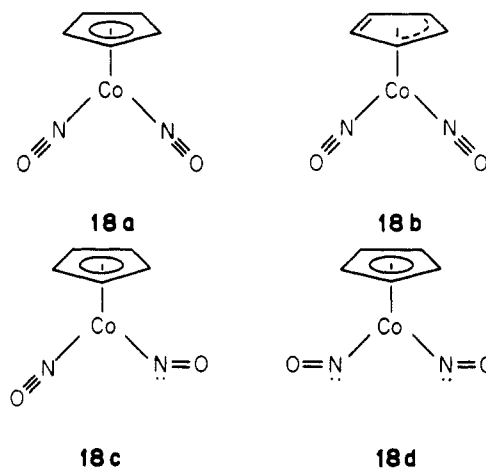


Figure 12 shows on the left side a Walsh diagram for a bending of **18a** to **18d** ( $\theta$  changes from  $180^\circ$  in **18a** to  $135^\circ$  in **18d**). It appears that both  $\pi^*_{\text{NO}}$  orbitals which are of  $p_z$  character are stabilized by the bending, whereas the other valence orbitals are unaffected. The unoccupied MO which decreases in energy by the bending is  $x^2-y^2$  on cobalt, out-of-phase with the  $p_x$ ,  $p_z$  combination on both nitrogens, whereas the HOMO which decreases is mainly  $yz$  on cobalt, out-of-phase with the  $p_x$ ,  $p_z$  combination on both nitrogens. The observed decrease in energy of the two

(28) Evrad, G.; Thomas, R.; Davis, B. R.; Bernal, I. J. *Organomet. Chem.* **1977**, *124*, 59.

(29) Hofmann, P. *Angew. Chem., Int. Ed. Engl.* **1977**, *16*, 536.

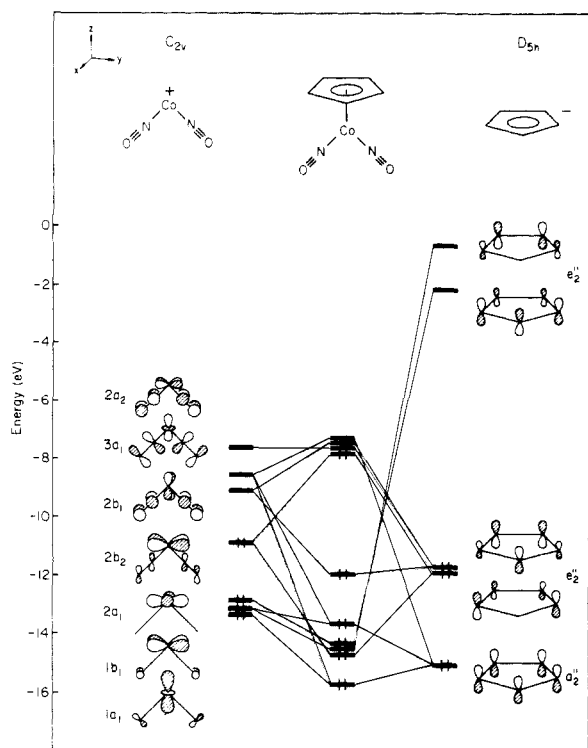


Figure 10. Interaction diagram for construction of "planar"  $\text{CpCo}(\text{NO})_2$  from the valence orbitals of  $\text{Co}(\text{NO})_2^+$  (left) and  $\text{C}_5\text{H}_5^-$  (right).

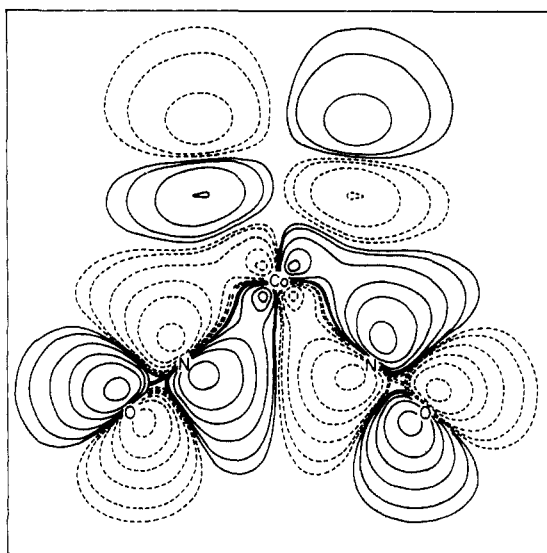


Figure 11. Contour plot of the HOMO in  $\text{CpCo}(\text{NO})_2$ . For contours and plane, see Figure 2.

levels is likely to be caused by a loss of antibonding overlap between metal and nitrosyl orbitals. This was confirmed by checking the appropriate fragment overlaps.

The stabilization of the HOMO indicates that a bent structure probably is more stable than the linear one. Calculation of the total one-electron energy for **18a**, **18c**, and **18d** gives that both **18c** (one nitrosyl bent) and **18d** (two nitrosyls bent) are more stable than **18a**. The energy minimum for **18c** is found for a bending of  $126^\circ$ , and this minimum is found to be about 0.2 eV lower than the minimum for **18d**, which appears at  $144^\circ$ .<sup>30</sup>

It appears from Figure 12 that the orbitals which change most in energy during the bending are just the orbitals which might

(30) It should be noted here that it has recently been shown by  $^{15}\text{N}$  NMR that there is a rapid intramolecular interconversion of bent and linear nitrosyl ligands in  $[\text{RuCl}(\text{NO})_2(\text{PPh}_3)_2]\text{BF}_4$  in solution. Mason, J.; Mingos, D. M. P.; Sherman, D.; Wardle, R. W. M. *J. Chem. Soc., Chem. Commun.* **1984**, 1223.

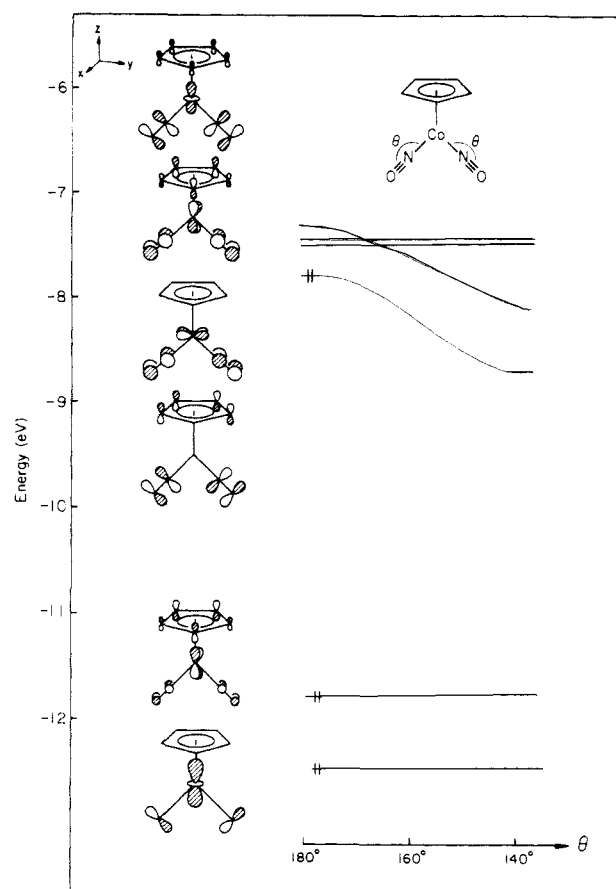


Figure 12. Walsh diagram for a symmetric bending of the two nitrosyls in  $\text{CpCo}(\text{NO})_2$ .

be expected to interact with the  $\pi$  and  $\pi^*$  orbitals of an alkene. We see the same trends here as in the case of the osmium oxide and imino frontier orbitals: the LUMO (in the bent state) is symmetric with respect to the  $xz$  plane, and the HOMO is antisymmetric with respect to the same plane. Thus, a favorable interaction with the HOMO and LUMO of an alkene is possible. Figure 13 shows the contours of the HOMO (**13a**) and LUMO (**13b**) wave functions of **18d** plotted in the  $yz$  plane.

The symmetric and antisymmetric pattern with respect to the  $xz$  plane is clear. These orbitals are perfectly set up to interact with an ethylene.

The frontier orbitals of **18c**, a single bent nitrosyl, not shown here in detail, are also well-arranged for interaction with an alkene. We cannot say from our approximate calculations which isomer, **18c** or **18d**, will be the reactive species. We will proceed with the analysis of **18d**, which is easier to carry through because the molecule has a mirror plane.

Incidentally, if one compares the orbitals of a carbonyl  $\text{CpCo}(\text{CO})_2$  with the present nitrosyl  $\text{CpCo}(\text{NO})_2$ , one finds that the carbonyl complex orbitals are not suitable for the cycloaddition either from an energy criterion or an overlap criterion.

The interaction diagram for the formation of a 1,2-dinitrosoethane complex from  $\text{CpCo}(\text{NO})_2$  and ethylene is shown in Figure 14. At the left side, the energy levels of  $\text{CpCo}(\text{NO})_2$  are shown; at the right are the levels of ethylene. In the center is the product of the reaction. The diagram has been constructed for the same orbitals of bent  $\text{CpCo}(\text{NO})_2$  as those shown in Figure 12. The HOMO and LUMO orbitals of  $\text{CpCo}(\text{NO})_2$  interact in the expected way with the ethylene fragment: The symmetric LUMO of  $\text{CpCo}(\text{NO})_2$  interacts with the symmetric HOMO of ethylene, and similarly the antisymmetric HOMO of  $\text{CpCo}(\text{NO})_2$  interacts with the antisymmetric LUMO of the ethylene. These interactions are, as the diagram indicates, stabilizing. After interaction, the  $xz$  orbital of  $\text{CpCo}(\text{NO})_2$  becomes the HOMO, and  $\pi^*_{\text{NO}}$  is the LUMO in the product.

When the above results are compared with the results obtained



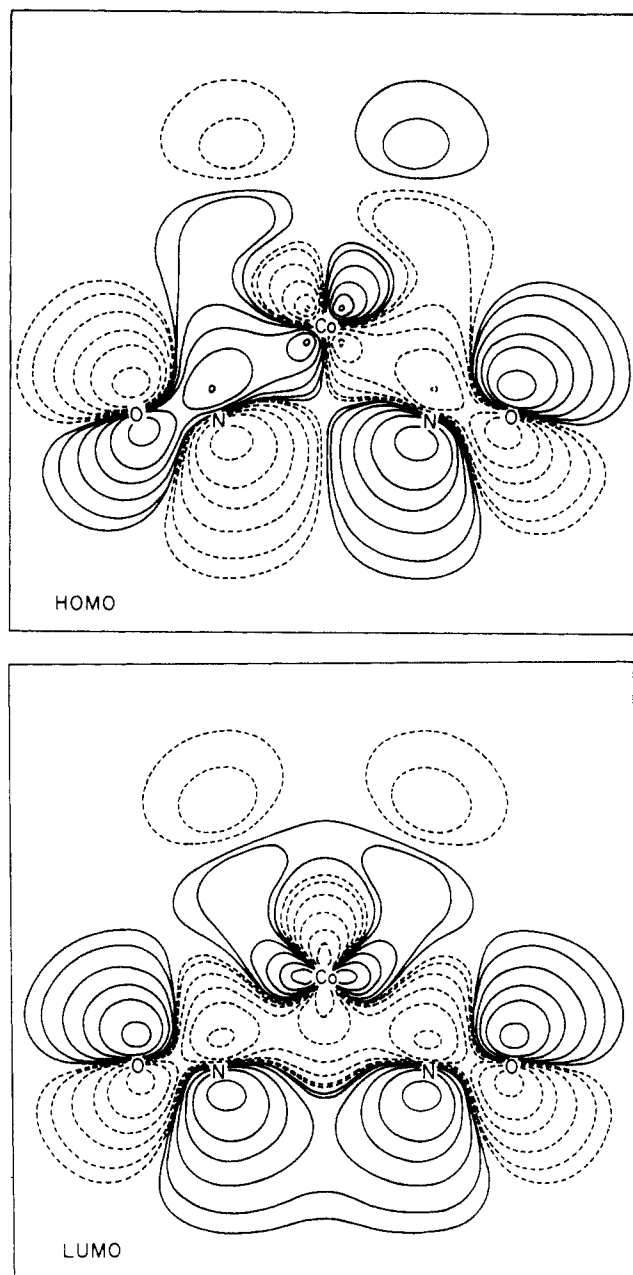


Figure 13. Contour plots of the HOMO and LUMO of 18d. For contours and plane, see Figure 2.

earlier in this paper in the study of ethylene binding to the ligands in the osmium complexes, it appears that the pattern is very similar. A [3 + 2] cycloaddition reaction seems the most probable reaction course here as well.

### Summary

We have tried to give a coherent theoretical model for the binding of alkenes to the ligands in osmium tetroxide, oxyiminoosmium complexes, and a seemingly very different ( $\eta^5$ -cyclopentadienyl)dinitrosocobalt complex. The frontier orbitals of osmium tetroxide have the right symmetry for an interaction with the  $\pi$  and  $\pi^*$  orbitals of an alkene. We have suggested that the increased reactivity of osmium tetroxide with alkenes in the presence of pyridine comes from a *cis* addition of pyridine to the metal center, causing a geometric distortion of osmium tetroxide from  $T_d$  to  $C_{2v}$  symmetry, in accordance with the structure of the isolated products in these reactions. From the present analyses, we tend to believe that the reaction proceeds as a concerted [3 + 2] cycloaddition; although we have not examined nor can rule out Sharpless's interesting suggestion of an asymmetric inter-

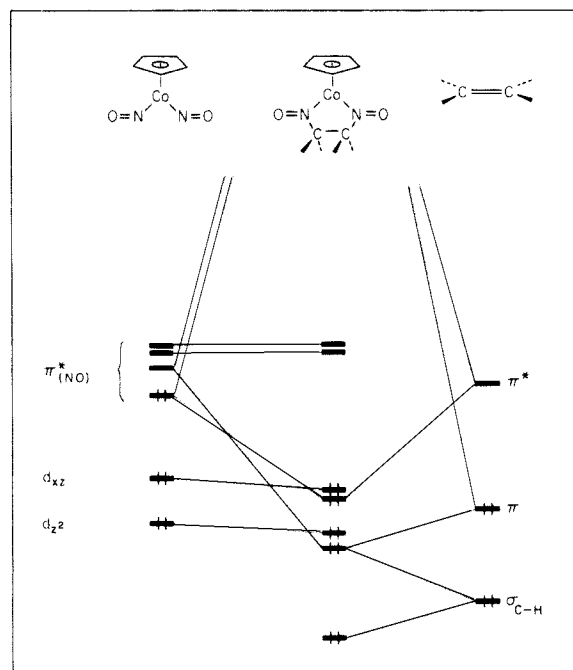


Figure 14. Interaction diagram for the orbitals of  $\text{CpCo}(\text{NO})_2$  (left) and ethylene (right). The product is in the center.

Table I. Parameters Used in Extended Hückel Calculations

orbital	$H_{ii}$	exponents	
		$\zeta_1^a$	$\zeta_2$
H 1s	-13.6	1.3	
C 2s	-21.4	1.55	
2p	-11.4	1.325	
N 2s	-26.0	1.875	
2p	-14.8	1.65	
O 2s	-32.3	2.20	
2p	-14.8	1.975	
Co 4s	-9.21	2.0	
4p	-5.29	2.0	
4d	-13.18	5.55 (0.555 08) <sup>a</sup>	1.9 (0.646 09)
Os 6s	-8.17	2.452	
6p	-4.81	2.429	
5d	-11.84	5.571 (0.637 17)	2.416 (0.559 82)
Ru 5s	-8.6	2.078	
5p	-3.28	2.043	
4d	-11.12	5.378 (0.534 03)	2.303 (0.636 46)

<sup>a</sup> Coefficients and exponents in a double- $\zeta$  expansion.

mediate. We also present a related analysis of the binding of alkenes of oxyiminoosmium complexes and find that the preferred oxyamination in the presence of pyridine comes from a geometric distortion of the osmium complex, leading to preferred binding of the alkene to oxygen and nitrogen.

The orbitals of the interesting ( $\eta^5$ -cyclopentadienyl)dinitrosocobalt complex have been constructed from a cobalt dinitrosyl cation and cyclopentadienyl fragments. Several different structures are possible for this complex, mainly depending on the structure of the nitrosyl ligands. From a Walsh diagram type analysis and calculations of the total energy for nitrosyl bending, the most probable structure is one in which one or two of the nitrosyls are bent. The frontier orbitals in the ( $\eta^5$ -cyclopentadienyl)dinitrosocobalt complex are set up for an interaction with an alkene in a similar way as the orbitals of osmium complexes.

**Acknowledgment.** Karl Anker Jørgensen is on leave from the Department of Chemistry, University of Aarhus, DK-8000, Aarhus C, Denmark. The stay for Karl Anker Jørgensen at Cornell was made possible by economic support from Thanks to Scandinavia, Inc. (especially Richard Netter) and the Danish National Science Research Council. We are grateful to members of our research group and especially Ralph Wheeler for fruitful

comments. Thanks are expressed to Eleanor Stagg for typewriting and to Jane Jorgensen for the drawings.

#### Appendix

All calculations were performed by using the extended Hückel method.<sup>14</sup> The orbital parameters along with the  $H_{ij}$  values are

summarized in Table I. The bond lengths and angles for the osmium compounds were taken from ref 7, 11, and 15. For  $\text{CpCo}(\text{NO})_2$ , the following structural data were used:  $\text{Co-Cp}(\text{center}) = 1.72 \text{ \AA}$ ;  $\text{Co-N} = 1.72 \text{ \AA}$ ;  $\text{N-O} = 1.25 \text{ \AA}$ ;  $\angle \text{NCoN} = 90^\circ$ . For ethylene bonded to  $\text{CpCo}(\text{NO})_2$ , the data are taken from ref 28.

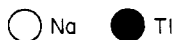
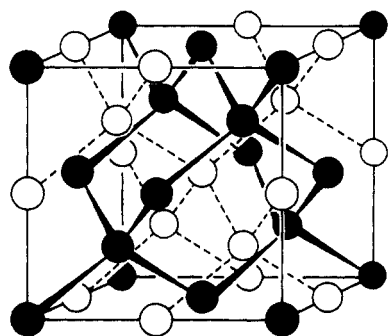
## Site Preferences and Bond Length Differences in $\text{CaAl}_2\text{Si}_2$ -Type Zintl Compounds

Chong Zheng,<sup>†</sup> Roald Hoffmann,<sup>\*†</sup> Reinhard Nesper,<sup>‡</sup> and Hans-Georg von Schnering<sup>\*†</sup>

Contribution from the Department of Chemistry and Materials Science Center, Cornell University, Ithaca, New York 14853, and Max-Planck-Institut für Festkörperforschung, D-7000 Stuttgart 80, FRG. Received September 16, 1985

**Abstract:** The  $\text{Al}_2\text{Si}_2^{2-}$  two-dimensional networks in the  $\text{CaAl}_2\text{Si}_2$  structure may be derived by a conceptual splitting of the wurtzite lattice and a subsequent reconstruction. The reconstruction suggests some analogies with organic propellanes. The resulting  $\text{Al}_2\text{Si}_2^{2-}$  network has two four-coordinate sites, a normal tetrahedral one, and another with a highly distorted local umbrella geometry. A choice is made by Al and Si for one or the other of these sites, a choice whose causes we explore in detail. We begin with a comparison of the energetics of the normal and the "inverted" phase, based on the dispersion of the bands. To avoid destabilizing high dispersion in the filled bands, the more electronegative atoms should occupy the less "dispersive" positions in the crystal. We also examine the Si-Al bonds of the  $\text{SiAl}_4$  "inverted" tetrahedron as isolated from and incorporated into the  $\text{CaAl}_2\text{Si}_2$  lattice. When an isolated  $\text{SiAl}_4^{8+}$  model is flipped from  $T_d$  to  $C_{3v}$  geometry, the 1-fold Si-Al bond is weakened more than the 3-fold bond. The reasons for this bring us again close to an organic propellane model. When the  $\text{SiAl}_4$  motif is incorporated into the lattice, additional inter-unit-cell interaction enhances the difference between the two types of Si-Al bonds. The possibility of an alternative "dimerized graphite"-type structure is also explored.

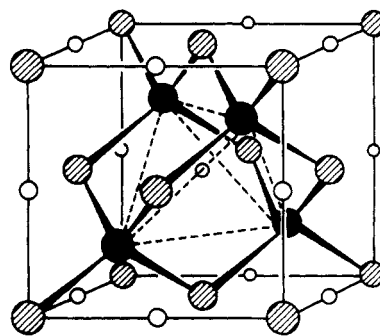
Zintl's concept<sup>1</sup> plays an important role in solid-state chemists' thinking and in their understanding of a large range of crystal structures. In this simple but extremely powerful concept, the electropositive elements are thought of merely as electron donors, donating electrons to the conjoined more electronegative element bonding partners. The latter then comply with the octet rule by receiving those electrons. An example is the  $\text{NaTl}$  structure,<sup>2</sup> 1, in which Na donates one electron to Tl, and the  $\text{Tl}^-$  moieties, isoelectronic to Pb, therefore similar to C, form the diamond structure. The  $\text{Na}^+$  cations build another diamond lattice, in-



1 NaTl

terpenetrating the  $\text{Tl}^-$  one. Closely related to the  $\text{NaTl}$  structure is the  $\text{LiAlSi}$  phase,<sup>3</sup> 2. Here the  $(\text{AlSi})^-$  network forms a

zinc-blende structure, and the  $\text{Li}^+$  ions sit in the center of the tetrahedra formed by the Si atoms.



2 LiAlSi

Though simple and most useful, Zintl's rule is not a universal predictor of molecular structure. It does not give us any hint as to why  $\text{NaAlSi}^4$  is not isostructural with  $\text{LiAlSi}$  or how the bond length should change when going from one structure to another. More sophisticated theoretical calculations are needed to explain

(1) See: Klemm, W. *Proc. Chem. Soc., London* **1958**, 329; Schäfer, H.; Eisenmann, B.; Müller, W. *Angew. Chem., Int. Ed. Engl.* **1973**, *12*, 694.

(2) Zintl, E.; Dullenkopf, W. *Z. Phys. Chem.* **1932**, *B16*, 195-205.

(3) (a) Schuster, H.-U.; Hinterkeuser, H.-W.; Schäfer, W.; Will, G. *Z. Naturforsch., B* **1965**, *31B*, 1540-1541. (b) Christensen, N. E. *Phys. Rev. B* **1985**, *32*, 6490.

(4) Westerhaus, W.; Schuster, H.-U. *Z. Naturforsch.* **1979**, *34B*, 352-353.

<sup>†</sup>Cornell University.

<sup>‡</sup>Max-Planck-Institut für Festkörperforschung.